JOURNAL OF THERMOPHYSICS AND HEAT TRANSFER
Vol. 23, No. 1, January–March 2009

Influence of a Streamwise Pressure Gradient on Film-Cooling Effectiveness

Kiran H. Dellimore,* Carlos Cruz,* Andre W. Marshall,† and Christopher P. Cadou†
University of Maryland, College Park, Maryland 20742

DOI: 10.2514/1.35717

Film cooling is widely used in conventional gas turbine and rocket engines to minimize thermal loading of engine structures and to manage heat transfer between hot, reacting gases and cooler structural components. Previous experimental work has shown that streamwise pressure gradients strongly influence the performance of the film. This paper extends semi-empirical modeling ideas for wall-jet film cooling to include the effects of adverse and favorable pressure gradients. The extended model shows that a pressure gradient's effect on cooling performance depends on whether the velocity of the film is greater than the core flow (a wall-jet film) or less than the core (a core-driven film). In wall-jet films, a favorable pressure gradient improves cooling performance by increasing the thickness and persistence of the film. Conversely, in core-driven films, a favorable pressure gradient reduces the persistence and thickness of the film leading to reduced cooling performance. Under isobaric conditions, the extended model results match experimental measurements within 2.5% in the near-slot region. When pressure gradients are present, the extended model matches experimental data to within 15% in the near-slot region and correctly predicts experimentally observed trends.

Nomenclature

a_0, C_0, N	=	constants
b	=	shear-layer thickness
b_0	=	film-cooling louver thickness
C_M	=	turbulent mixing coefficient
$C_{P\infty}$	=	hot-gas stream pressure coefficient
c	=	ratio of density in mixing zone I at the transition point to the coolant-stream density
I_v	=	overall average turbulence intensity
$I_{v,s}$	=	average transverse coolant-stream turbulence intensity
$I_{v,\infty}$	=	average transverse hot-stream turbulence intensity
K_p	=	Kays's acceleration parameter
M	=	blowing ratio, $(\rho_s U_s)/(\rho_\infty U_\infty)$
$\dot{m}'_e$	=	entrained hot-gas stream rate per unit length
$\dot{m}_f$	=	total mass flow rate of the film per unit length
$\dot{m}_s$	=	coolant mass flow rate per unit length
P	=	static pressure
p/d	=	hole spacing
R	=	ratio of the average hot-stream velocity to the average coolant-stream velocity, U_∞/U_s
R_0	=	ratio of the initial average hot-stream velocity to the initial average coolant-stream velocity, $U_{0\infty}/U_{0s}$
s	=	louver slot height
T	=	absolute temperature
U	=	average fluid stream velocity
x	=	streamwise distance
x_0	=	streamwise location of the point of coolant injection
x_1	=	streamwise location of the transition point between the initial and fully developed regions
y	=	transverse distance
y_1	=	transverse location of the shear-layer/coolant-stream interface
y_2	=	transverse location of the shear-layer/hot-stream interface
β	=	initial region factor
η_{eff}	=	film-cooling effectiveness, $(T_\infty\text{-}T_{\text{aw}})/(T_\infty\text{-}T_s)$
μ	=	dynamic viscosity
ρ	=	fluid density
ψ	=	dimensionless temperature ratio
ω	=	dimensionless flow-temperature grouping

Subscripts

aw	=	adiabatic wall
s	=	coolant stream
0	=	injection conditions
I	=	zone I of shear layer
II	=	zone II of shear layer
∞	=	hot-gas stream

Presented as Paper 5004 at the 43rd AIAA/ASME/SAE/ASEE Joint Propulsion Conference and Exhibit, Cincinnati, OH, 8–11 July 2007; received 16 November 2007; revision received 15 September 2008; accepted for publication 16 September 2008.

*Graduate Student, Department of Aerospace Engineering. AIAA Student Member.

†Associate Professor, Department of Aerospace Engineering. AIAA Senior Member.

I. Introduction

FILM cooling is an active cooling strategy commonly used in gas turbine and rocket engines to minimize thermal loading of engine structures and to manage heat transfer between hot, reacting gases and cooler structural components. Among its many advantages is that it allows combustors to operate at higher temperatures, thereby improving their thermal efficiency and reducing thermally induced mechanical stresses that shorten the life cycles of engine components. However, achieving effective film cooling is extremely challenging due to the inherently complex combustor flowfields and the wide array of geometric and fluid dynamic parameters that can affect film-cooling performance [1].

Previous work has shown that one of the key fluid dynamic factors affecting film-cooling effectiveness is the presence of a mainstream pressure gradient [2]. However, the results of several experimental and theoretical investigations [3–7] of the influence of a mainstream pressure gradient are often contradictory. For example, a comprehensive review by Teekaram et al. in 1989 [3] suggests that pressure gradients can either improve or degrade film-cooling performance depending upon the geometry. Two-dimensional slot

injection studies by Hartnett et al. [4] and Pai and Whitelaw [5] suggest that the influence of the pressure gradient is limited, as they showed that a favorable pressure gradient results in only a small decrease in the film-cooling effectiveness relative to zero-pressure gradient conditions. Pai and Whitelaw also showed that the influence of the pressure gradient depends on the distance from the slot, as well as the coolant to mainstream velocity and density ratios. In contrast, Hay et al.'s [6] investigation of film cooling through three-dimensional holes showed that mainstream pressure gradients have a strong influence on film-cooling effectiveness, particularly at low blowing ratios and in the vicinity of coolant injection. They reported a 70–80% reduction in the heat transfer coefficient in the presence of a strong favorable pressure gradient that corresponds to an acceleration parameter K_p of 5×10^{-6} at the point of injection. They found no significant effect on the heat transfer coefficient when the pressure gradient was mildly adverse ($K_p = -0.85 \times 10^{-6}$). Finally, Kruse's [7] investigations of film cooling downstream of a single row of discrete circular holes over a range of blowing ratios and injection angles concluded that adverse pressure gradients improve film-cooling effectiveness slightly, whereas favorable pressure gradients degraded film-cooling performance. Kruse also noted that the influence of the pressure gradient on film-cooling effectiveness was most pronounced when the blowing ratio and hole spacing were small.

There are relatively few analytical investigations of film-cooling performance. Goradia and Colwell [8] used superposition theory to develop a model for the effect of a streamwise pressure gradient on the growth of a wall-jet film without heat transfer. They compared the model's predictions to measurements in a two-dimensional turbulent wall-jet film over a range of velocity ratios in the presence of adverse and favorable pressure gradients, but found that their model was not reliable in the initial jet region. Simon [9] developed an incompressible, zero-pressure gradient, semi-empirical film-cooling model based on Abramovich's free shear-layer growth analysis [10]. The model incorporated turbulence and heat transfer and therefore was capable of accounting for the effects of freestream and coolant turbulence on film-cooling performance. Separate semi-empirical models for turbulent mixing in the developing and fully developed portions of the flow were used. The model's predictions matched experimental measurements of film-cooling effectiveness to within $\pm 4\%$ for lateral freestream turbulence intensities up to 24% and blowing ratios up to 1.9. Neither of these investigations account for the effect of mainstream pressure gradients.

The present work extends Simon's analysis [9] to account for the effect of mainstream pressure gradients on film-cooling performance. The predictions of the resulting modified Simon model (MSM) under isobaric conditions are compared with those of Simon's original model and to experimental measurements by Cruz et al. [11]. The MSM's predictions under nonisobaric conditions are compared with measurements from Teekaram et al. [3]. The comparison provides a clearer picture of the influence of mainstream pressure gradients on film cooling and resolves some of the conflicts in the open literature.

II. Analysis

Figure 1 is a schematic illustration of the wall-jet film-cooling situation investigated by Simon [9] but with the addition of a streamwise pressure gradient. The figure shows a coolant stream at a temperature T_s and velocity U_s being injected near the wall from a slot of height s. At x_0, the coolant stream encounters a hot-gas stream of temperature T_∞ (with $T_\infty > T_s$), moving at a velocity U_∞, where $U_\infty < U_s$. Associated with this hot-gas stream is a pressure gradient of magnitude $\mathrm{d}P/\mathrm{d}x$. A weakly turbulent shear layer of thickness b develops and grows with streamwise distance x at the interface between the coolant and hot-gas streams. The length of the initial developing region x_1 is taken to be the distance required for the inner edge of the developing mixing zone, labeled zone I in Fig. 1, to reach the wall. The initial developing region is often termed the "potential core" region and has been shown experimentally to provide very effective protection [12]. Following the approach of Simon [9], the adiabatic wall temperature in the initial region ($x < x_1$) T_{aw} is assumed to equal the mean fluid temperature in zone II (coolant zone), whereas, in the developed region, the adiabatic wall temperature is assumed to equal the mean fluid temperature in zone I. Hence,

$$T_{\mathrm{aw}} = \begin{cases} \bar{T}_{\mathrm{II}}, & (x < x_1) \\ \bar{T}_{\mathrm{I}}, & (x \geq x_1) \end{cases} \tag{1}$$

The following assumptions are also made:

1) The change in the specific heat with temperature is small.
2) The composition of the coolant and hot streams is the same.
3) The hot-gas stream temperature T_∞ is constant.
4) Thermal radiation from the hot-gas stream is negligible.
5) The shear-layer growth b is linear.

A. Film-Cooling Model Development

Film-cooling effectiveness η_{eff} is typically defined for an incompressible flow as [13]

$$\eta_{\mathrm{eff}} = \frac{T_\infty - T_{\mathrm{aw}}}{T_\infty - T_s} \tag{2}$$

From a mass and energy balance on the coolant stream, it can be shown, following Stollery and El-Ehwany [14], that the film-cooling effectiveness is related to the amount of hot-stream gas entrained by the coolant stream:

$$\eta_{\mathrm{eff}} = \frac{\dot{m}_s}{\dot{m}_f} \tag{3}$$

where $\dot{m}_s$ is the coolant mass flow rate per unit length, $\dot{m}_s = \rho_s U_s s$, and $\dot{m}_f$ is the total mass flow rate of the film per unit length, at any arbitrary x location downstream of the coolant slot exit. The value of $\dot{m}_f$ includes both the coolant mass flow rate per unit length and the entrained hot-gas stream rate per unit length $\dot{m}'_e$. This can be expressed as follows:

$$\dot{m}_f = \dot{m}_s + \int_0^x \dot{m}'_e \, \mathrm{d}x \tag{4}$$

Following the approach of Juhasz and Marek [13], $\dot{m}'_e$ is assumed to be directly proportional to the hot-gas stream mass flux:

$$\dot{m}'_e = C'_M \rho_\infty U_\infty \tag{5}$$

where C'_M is an "effective" turbulent mixing coefficient, which is related to the average turbulence intensity I_v.

Substitution of Eqs. (4) and (5) into Eq. (3) yields

$$\eta_{\mathrm{eff}} = \left[1 + \left(\frac{x}{Ms} \right) C'_M \right]^{-1} \tag{6}$$

where M is the blowing ratio (defined as the ratio of the coolant stream to hot-stream mass flux):

$$M = \frac{\rho_s U_s}{\rho_\infty U_\infty} \tag{7}$$

Equation (6) gives the functional form for a basic turbulent film-cooling correlation. It shows that film-cooling effectiveness decreases with increasing streamwise distance, with decreasing blowing ratio, with decreasing slot height, and with increasing turbulence intensity.

Following Simon's [9] approach, C'_M is written in terms of the turbulent mixing coefficient C_M and a turbulent diffusion parameter β:

$$C'_M = \frac{C_M - \beta (x/Ms)^{-1}}{1 + \beta} \tag{8}$$

The parameter β accounts for turbulent diffusion from zone I to zone II in the initial region ($x < x_1$) only. It therefore has a value of

zero in the developed region ($x \geq x_1$). C_M is a function of the shear-layer entrainment rate db/dx, which can be directly related to I_v using Abramovich's [10] empirical assumption that db/dx is proportional to the perturbation component of the fluctuating hot-gas stream velocity v_0'. This leads to

$$C_M = \frac{db}{dx} = \frac{a_0 v_0'}{U_0^*} \tag{9}$$

where a_0 is an empirical constant and U_0^* is the characteristic velocity of the shear layer given by

$$U_0^* = \frac{\rho_\infty U_\infty + \rho_s U_s}{\rho_\infty + \rho_s} \tag{10}$$

Substituting Eq. (10) into Eq. (9), simplifying by noting that $I_v = v_0'/U_\infty$, and incorporating Eq. (7) yields an expression for C_M, which in general form can be written as

$$C_M = a_0 (I_v \omega)^N \tag{11}$$

In this expression, N is an empirically determined constant, ω is a dimensionless flow-temperature parameter developed by Simon [9], and I_v is the overall average transverse turbulence intensity. I_v and ω are given by

$$I_v = I_{v,\infty} + 0.4(|I_{v,\infty} - I_{v,s}|) \tag{12}$$

$$\omega = \frac{(1 + 1/\mathrm{TR})}{(1 + M)} \tag{13}$$

where TR is the temperature ratio, which is defined as the ratio of the coolant to hot-stream static temperature T_s/T_∞. $I_{v,s}$ is the initial average transverse coolant-stream turbulence intensity, and $I_{v,\infty}$ is the initial average transverse turbulence intensity of the hot-gas stream; I_v is based on a turbulent correlation obtained from Ko and Liu [15], which has the constraint that I_v cannot be greater than either $I_{v,\infty}$ or $I_{v,s}$. Equation (11) is used by Simon [9] to account for turbulence in both the initial region ($x < x_1$) and in the developed region ($x \geq x_1$).

Returning to the β parameter from Eq. (8), Simon [9] developed the following expression for β based on empirical observation and by noting that the turbulent diffusion from zone I to zone II is a function of the initial average transverse turbulence intensity of the coolant stream $I_{v,s}^*$:

$$\beta = \left[C_M \left(\frac{x}{Ms} \right) + \left(\frac{x}{x_1} \right) - C_0 I_{v,s}^* \left(\frac{T_s}{T_{\mathrm{aw}_{x=x1}}} \right) \ell_n \left(\frac{1}{1 - (x/x_1)} \right) \right] \left(\frac{T_{\mathrm{aw}_{x=x1}} - T_{\mathrm{aw}}}{T_\infty - T_s} \right) \tag{14}$$

In Eq. (14), C_0 is an empirically determined constant.

The location of the transition point between the initial and fully developed regions x_1 can be determined from the geometry of the shear layer, as shown in Fig. 1, to be

$$x_1 = \frac{s}{y_1} x \tag{15}$$

where y_1 is the shear-layer/coolant-stream interface position.

Next, by noting from Fig. 1 that the shear-layer thickness $b = y_1 + y_2$, and that the turbulent mixing coefficient C_M is related to the shear-layer growth rate by $C_M = (b - y_1)/x$, Eq. (15) can be simplified to

$$x_1 = \left[\left(\frac{C_M}{s} \right) \frac{y_1}{y_2} \right]^{-1} \tag{16}$$

where y_2 is the shear-layer/hot-stream interface position.

Before proceeding further, it is important to note that the introduction of a pressure gradient does not change the forms of Eqs. (1–14), as the pressure gradient has no effect on the mass or energy balance in zones I or II. However, the pressure gradient does affect the momentum balance in zones I and II, thereby influencing the location of the transition point between the initial and fully developed regions through y_1/y_2 in Eq. (16). So, the next step is to use Abramovich's [10] semi-empirical theory of incompressible, turbulent jets (or shear layers) to find y_1/y_2. Once y_1/y_2 is known, x_1 can be determined using Eq. (16), and the streamwise evolution of film-cooling effectiveness can be computed using Eq. (6) plus Eqs. (7–14).

B. Isobaric Case

Abramovich [10] showed that, for an incompressible shear layer formed between two coflowing streams of different velocities in the absence of a pressure gradient, the shear-layer growth rate can be expressed as

$$\frac{db}{dx} = k \tag{17}$$

where β is the shear-layer thickness and k is a constant which depends on R, the ratio of the average hot-stream velocity to the average coolant-stream velocity ($R \equiv \bar{U}_\infty/\bar{U}_s$):

$$k = \pm c \frac{1 - R}{1 + R} \tag{18}$$

where c is a constant which represents the density ratio between the two streams. The negative sign is taken when $R > 1$, that is, when $U_\infty > U_s$. This corresponds to a core-driven film situation. Integrating Eq. (17) yields the following expression for the shear-layer thickness:

$$b = \pm c \left(\frac{1 - R}{1 + R} \right) x \tag{19}$$

Equation (19) shows that the growth in the shear-layer thickness b in the absence of a pressure gradient depends only on the velocity and density ratio. It also shows that the shear-layer thickness varies linearly with streamwise distance. This expression can be related to Eq. (16), by performing a momentum and mass balance on the two streams to obtain an expression for y_1/b. This has been done previously by Abramovich [10] and yields the following result:

$$\frac{y_1}{b} = c(0.416 + 0.134R) \tag{20}$$

Recalling that $b = y_1 + y_2$ (see Fig. 1), Eq. (20) can be rearranged to obtain an expression for y_1/y_2:

$$\frac{y_1}{y_2} = \left(\frac{1}{c(0.416 + 0.134R)} - 1 \right)^{-1} \tag{21}$$

Following the approach of Simon [9], c is defined to be the ratio of the fluid density in mixing zone I at the transition point x_1 to the coolant-stream density:

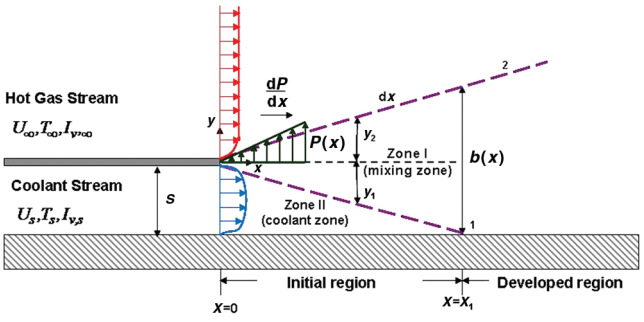

Fig. 1 Wall-jet film-cooling model with a pressure gradient adapted from Simon [9] (1986).

$$c = \frac{T_s}{T_{\mathrm{aw}_{x=x1}}} \tag{22}$$

Equations (21) and (22) combined with Eqs. (1–16) form the Simon model (SM) [9] which is valid for wall-jet film cooling in the absence of a pressure gradient.

C. Nonisobaric Case

An analogous approach is used to develop an expression for y_1/y_2 under nonisobaric conditions. Returning to the semi-empirical theory of incompressible, turbulent jets (or shear layers), if a longitudinal mainstream pressure gradient is present, as shown in Fig. 1, it can be shown using Bernoulli's equation that the ratio of the local hot-stream velocity at a given x location U_∞ to the initial hot-stream velocity $U_{0\infty}$ along an arbitrary streamline is given by

$$\frac{U_\infty^2}{U_{0\infty}^2} = 1 - \left[\frac{P_\infty(x) - P_{0\infty}}{\frac{1}{2}\rho U_{0\infty}^2}\right] \tag{23}$$

where $P_\infty(x)$ is the local hot-stream static pressure at a given x location, and $P_{0\infty}$ is the static pressure of the hot stream at the point of coolant injection.

Noting that the pressure coefficient (nondimensional pressure gradient) $C_{P\infty}$ is defined as

$$C_{P\infty} = \frac{P_\infty(x) - P_{\infty,x=0}}{\frac{1}{2}\rho \bar{U}_{\infty,x=0}^2} \tag{24}$$

where $C_{P\infty} > 0$ corresponds to an adverse pressure gradient, and $C_{P\infty} < 0$ corresponds to a favorable pressure gradient.

We can simplify Eq. (23) by substituting Eq. (24) and by introducing definitions for the local hot-stream to coolant-stream velocity ratio R, that is, $R = U_\infty/U_s$, and for the initial hot-stream to coolant-stream velocity ratio R_0, that is, $R_0 = U_{0\infty}/U_{0s}$. This leads to an expression for R in terms of R_0 and $C_{P\infty}$which is given by

$$R = \sqrt{\left(\frac{R_0^2 - C_{P\infty}}{1 - C_{P\infty}}\right)} \tag{25}$$

Substituting Eq. (25) into Eqs. (17) and (18) and simplifying leads to an expression for the shear-layer growth rate that is analogous to the growth rate expression for the isobaric case:

$$\frac{\mathrm{d}b}{\mathrm{d}x} = k' + \ell \tag{26}$$

The first term, k', corresponds directly to k in the isobaric case [Eq. (17)] and is given by

$$k' = \pm c\frac{1 - R_0}{1 + R_0} \tag{27}$$

The second term, ℓ, is new and arises because of the pressure gradient. It is given by

$$\ell = 2c\frac{R_0 - C_{P\infty} - \sqrt{(1 - C_{P\infty})(R_0^2 - C_{P\infty})}}{1 - R_0^2} \tag{28}$$

As in the isobaric case, the negative sign in Eq. (27) is taken for a core-driven film (i.e., $R_0 > 1$) and the positive sign is taken for a wall jet.

An expression for the shear-layer thickness is obtained by integrating Eq. (26). Applying the boundary condition that, at $x = 0$, $b = 0$ yields the following expression for the variation of the shear-layer thickness with x:

$$b = \pm cx\frac{1 - R_0}{1 + R_0} \mp \frac{cx}{1 - R_0^2}\left\{R_0 - \frac{1}{2}C_{P\infty} - \frac{1}{4C_{P\infty}}[(2C_{P\infty} - 1 - R_0^2)\sqrt{K_1} + R_0(1 + R_0^2) - 2(1 - R_0^2)\,\ell_n\,|K_2|]\right\} \tag{29}$$

$$K_1 = (1 - C_{P\infty})(R_0^2 - C_{P\infty}) \tag{30}$$

$$K_2 = \frac{1 + R_0^2 - 2C_{P\infty} - 2\sqrt{K_1}}{1 - R_0^2} \tag{31}$$

Equations (29–31) show that the shear-layer thickness is a function of R_0, $C_{P\infty}$, and x. As in the isobaric case, Abramovich [10] performed a mass and momentum balance on the two streams to obtain an expression for y_1/b:

$$\frac{y_1}{b} = \frac{(1 - C_{P\infty})(0.416 + 0.268R + 0.316R^2) - R_0\sqrt{1 - C_{P\infty}}(0.55 + 0.45R) + 2C_{P\infty} - (1 - R_0)(1 - \sqrt{1 - C_{P\infty}})(b_0/b)}{(1 - R_0)\sqrt{1 - C_{P\infty}}} \tag{32}$$

Substituting Eqs. (25), (29), and (30) into Eq. (32) and recalling that $b = y_1 + y_2$ (see Fig. 1) gives an expression for y_1/y_2:

$$\frac{y_1}{y_2} = \frac{1}{\frac{1}{c[(2C_{P\infty}/\sqrt{1-C_{P\infty}}) + \sqrt{1-C_{P\infty}}\{0.416 + [0.316K_1/(1-C_{P\infty})^2] + 0.268(\sqrt{K_1}/1-C_{P\infty})\} - R_0[0.55 + 0.45(\sqrt{K_1}/1-C_{P\infty})] - K_3]} - 1} \tag{33}$$

$$K_3 = \frac{b_0(1 - R_0 - R_0^2 + R_0^3)(-1 + 1/\sqrt{1 - C_{P\infty}})}{c[(1 - R_0)^2 x - (R_0 x - C_{P\infty}x/2 - b_0/4s\{R_0(1 + R_0^2) + (-1 - R_0^2 + 2C_{P\infty})\sqrt{K_1} + [-2(1 - R_0^2)\,\ell_n\,|K_2|]\})]} \tag{34}$$

Using Eqs. (33) and (34) to represent $y1/y2$ in Eqs. (1–16) gives the modified Simon model, which is valid for incompressible, film cooling in the presence of a mainstream pressure gradient. In the limit as $C_{P\infty} \to 0$, Eqs. (33) and (34) simplify to give

$$\frac{y_1}{y_]} = \left(\frac{1}{[c/(1 - R_0)][0.416 - 0.282R_0 - 0.134R_0^2]} - 1\right)^{-1} \tag{35}$$

Factoring this equation and noting from Eq. (25) that, when the pressure gradient tends to zero, $R_0 \to R$ yields

$$\frac{y_1}{y_2} = \left(\frac{1}{c(0.416 + 0.134R)} - 1\right)^{-1} \tag{36}$$

Equation (36) is identical to Eq. (21). Therefore, when the pressure gradient is zero, the MSM predicts exactly the same film-cooling effectiveness as the SM.

III. Choosing Values for the Model's Parameters

To apply the film-cooling model developed in Sec. II, one must select values for the model's empirical parameters C_0, a_0, and N. In addition, the model also requires inputs for the initial coolant-stream and hot-stream turbulence intensities, $I_{v,s}$ and $I_{v,\infty}$, which historically have not be reported in previous experimental work in the open literature. Film-cooling data from Cruz et al. [11] and Teekaram et al. [3] were used to validate the model's predictions under zero-pressure gradient and variable pressure gradient conditions, respectively.

Cruz et al. [11] reported film-cooling effectiveness as a function of downstream distance x in a subsonic hot-wind-tunnel facility. A wall-jet flow condition was used for model validation, having a hot-stream velocity of 20.0 m/s at a temperature of 431 K and a coolant-stream velocity of 31.5 m/s at a temperature of 306 K. Laser Doppler velocimetry measurements indicated that the average coolant-stream turbulence intensity $I_{v,s}$ was 5.0%, whereas the average hot-stream turbulence intensity $I_{v,\infty}$ was 1.6%. A sensitivity analysis showed that the MSM model is insensitive to the value of C_0, and so it was simply set to the value used by Simon [9] ($C_0 = 13.7$) for both the isobaric and variable pressure gradient cases. A two-variable least-squares analysis was used to find the values of the remaining model parameters N and a_0. The analysis found that choosing $N = 0.8592$ and $a_0 = 0.4950$ produced the best correspondence between the model and the experimental results. Figure 2 shows that, with these assumptions, the SM (solid lines) and the MSM (dashed lines) predict the experimentally measured film-cooling efficiency (symbols) to within 2.5% of the experimentally measured values in the near-slot region ($x/Ms < 30$). The models do not perform as well farther downstream of the slot but are consistent with the data trend.

Teekaram et al. [3] measured film-cooling effectiveness under variable pressure gradient conditions using an isentropic light piston tunnel facility. Various contoured nozzles were used to produce adverse and favorable pressure gradients that varied with downstream distance. The hot-stream flow Mach number was maintained between 0.5 and 0.6 at a static temperature of 348 K. The coolant injection Mach number was varied from 0.07 to 0.34 at a static temperature of 295 K. This approach allowed blowing ratios between 0.15 and 0.75 to be achieved. Acceleration parameters ranging from $K_p = 2.62 \times 10^{-6}$ (favorable pressure gradient) to -0.22×10^{-6} (adverse pressure gradient) were achieved at the point of coolant injection. The average hot-stream and coolant-stream turbulence intensities were not reported in this study, and so it was necessary to estimate $I_{v,\infty}$ and $I_{v,s}$, in addition to N and a_0. Since $I_{v,\infty}$ and $I_{v,s}$ can be expressed as a single variable I_v using Eq. (13), a three-variable least-squares (LSQ) analysis was performed to find the values of a_0, N, and I_v that provided the best correspondence between the MSM predictions and Teekaram's experimental measurements under zero-pressure gradient conditions. However, the values obtained for a_0, N, and I_v were very sensitive to the initial guesses for I_v, N, and a_0. Some initial guesses even led to nonphysical values of I_v and no reliable results were obtained using this method. As a result, an alternate strategy was embraced in which a two-variable least-squares analysis was performed to determine values of a_0 and N, over a range "reasonable" values of I_v (i.e., $1 \le I_v \le 5\%$). The results of this procedure are summarized in Table 1 and show that similar levels of agreement between the zero-pressure gradient measurements of Teekaram et al. and the MSM can be obtained for a wide range of different combinations of a_0, N, and I_v. The residuals are the smallest and approximately constant for values of I_v between 0.015 and 0.030. Values of a_0, N, and I_v, equal to 0.4474, 0.8738, and 0.020, respectively, give the smallest residual, and so these values were chosen to compare the MSM's predictions to the experimental data. Because many different combinations of $I_{v,s}$ and $I_{v,\infty}$ can produce the same value of I_v, for simplicity, $I_{v,s}$ and $I_{v,\infty}$, are assumed to be equal.

Table 1 Summary of empirical constants determined for the ZPG Teekaram et al. [3] data

I_v	A_0	N	Residual	LSQ method
0.010	0.026517	0.002113	0.146568	2 variable
0.015	0.0706	0.3108	0.120210	2 variable
0.020	**0.4474**	**0.8738**	**0.120085**	**2 variable**
0.025	1.8411	1.3802	0.120356	2 variable
0.030	3.4775	1.6662	0.120172	2 variable
0.035	0.1770	0.6500	0.161288	2 variable
0.040	0.177	0.65	0.194657	2 variable
0.045	0.0893	0.5786	0.141179	2 variable
0.050	0.075502	0.457653	0.124767	2 variable

Figure 3 compares film-cooling effectiveness predicted by the MSM (solid lines) assuming $I_{v,s}$ and $I_{v,\infty}$ are both 0.02 (i.e.. $I_v = 0.02$) to experimental measurements from Teekaram et al. [3] under isobaric conditions. The shaded region illustrates the range of values of η_{eff} predicted by the MSM for values of I_v between 0.01 and 0.05. The predictions of the MSM appear to be in good agreement with the experimental data over the entire range of I_v values. Therefore, we conclude that the predictions of the MSM are not overly sensitive to the choice of I_v and that this fitting procedure is reasonable when average values of I_v are not available.

IV. Results

A. Constant Pressure Gradient Case

1. *Wall-Jet Film*

Figure 4 is a plot of film-cooling effectiveness predicted by the MSM as a function of nondimensional downstream distance for a turbulent wall-jet film in the presence of three different pressure gradients. The dashed line corresponds to a favorable pressure gradient ($C_{P\infty} = -0.05$), the dotted line to an adverse pressure gradient ($C_{P\infty} = +0.05$), and the solid line to the isobaric case

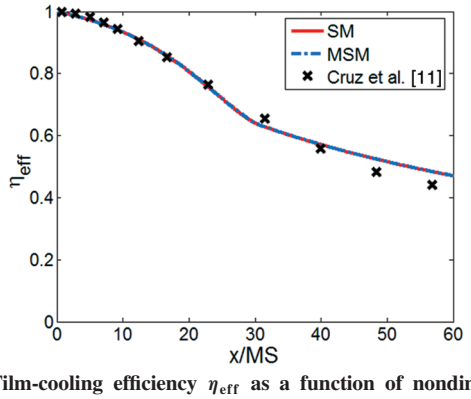

Fig. 2 Film-cooling efficiency η_{eff} as a function of nondimensional streamwise distance x/Ms for an isobaric, turbulent wall-jet film ($R = 0.63$) at $M = 2.22$ and TR = 0.71, as predicted by the SM and MSM.

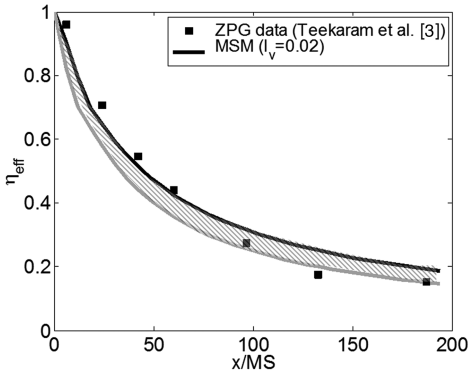

Fig. 3 Comparison of film-cooling efficiency η_{eff} as a function of nondimensional streamwise distance, x/Ms, predicted by the MSM to experimental measurements by Teekaram et al. [3] for a turbulent core-driven film ($R_0 = 3.53$) in the presence of a constant zero-pressure gradient, at $M = 0.33$, TR = 0.86.

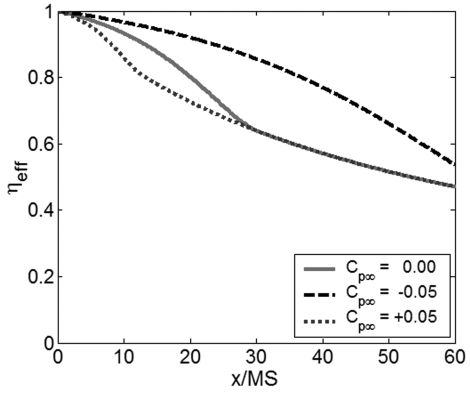

Fig. 4 Film-cooling efficiency η_{eff} as a function of nondimensional streamwise distance x/Ms for a turbulent wall jet ($R_0 = 0.63$) undergoing a constant favorable pressure gradient ($C_{P\infty} = -0.05$), a constant adverse pressure gradient ($C_{P\infty} = +0.05$), and a constant zero-pressure gradient ($C_{P\infty} = 0.0$), at $M = 2.22$ and TR $= 0.71$, as predicted by the MSM.

($C_{P\infty} = 0.0$). The results show that, for a wall-jet film, the presence of an adverse pressure gradient decreases film-cooling efficiency (in this case by as much as 12.5%). In contrast, a favorable pressure gradient increases the cooling effectiveness (in this case by as much as 30%).

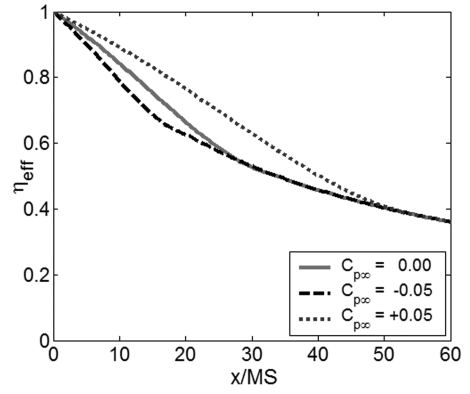

Fig. 5 Film-cooling efficiency η_{eff} as a function of nondimensional streamwise distance x/Ms for a turbulent core-driven film ($R_0 = 1.58$) undergoing a constant favorable pressure gradient ($C_{P\infty} = -0.05$), a constant adverse pressure gradient ($C_{P\infty} = +0.05$), and a constant zero-pressure gradient ($C_{P\infty} = 0.0$), at $M = 0.89$ and TR $= 0.71$, as predicted by the MSM.

2. Core-Driven Film

Figure 5 is a plot of film-cooling effectiveness predicted by the MSM as a function of nondimensional downstream distance for a turbulent core-driven film in the presence of three different pressure gradients. The dashed line corresponds to a favorable pressure gradient ($C_{P\infty} = -0.05$), the dotted line to an adverse pressure gradient ($C_{P\infty} = +0.05$), and the solid line to the isobaric case ($C_{P\infty} = 0.0$). Figure 5 shows that the behavior observed reverses for a core-driven film. In this case, the presence of a favorable pressure gradient decreases the film-cooling efficiency by as much as 10%. Meanwhile, the presence of an adverse pressure gradient actually increases the film-cooling effectiveness (in this case by as much as 20%). Taken together, Figs. 4 and 5 show that the effect of the pressure gradient reverses depending on whether $R > 1$ or $R < 1$. This is important because it helps to explain some seemingly contradictory results in the literature. This will be addressed later. For the moment, let us consider why this reversal occurs.

3. Explanation for Reversed Effect of $C_{P\infty}$

Figure 6 shows the shear-layer thickness at the impingement point, $b(x_1)/s$, as a function of the initial region length x_1/s and the pressure gradient $C_{P\infty}$ for a wall-jet film (dotted line) and a core-driven film (solid line). The figure shows that applying a favorable pressure gradient ($C_{P\infty} < 0$) to a wall-jet film ($R < 1$) increases the length of the initial region as well as the thickness of the shear layer. The increase in x_1/s means that more of the wall is protected, and an increase in $b(x_1)/s$ means that the hot freestream moves farther away from the wall. These effects combine to improve film-cooling performance. In contrast, when a favorable pressure gradient is applied to a core-driven film ($R > 1$), x_1/s is reduced, which means less of the wall is protected and $b(x_1)/s$ decreases, which means that the hot flow is closer to the wall. Together, these effects degrade cooling performance. The figure also shows that reducing the slot height s degrades performance in both types of jets by decreasing the length of the protected region and decreasing the thickness of the shear layer.

But why do the changes in x_1/s and $b(x_1)/s$ with $C_{P\infty}$ depend on whether $R_0 > 1$ or $R_0 < 1$? Equation (26) shows that the shear-layer growth rate is the sum of two terms: a term k' that depends on the velocity ratio alone [Eq. (27)] and a term ℓ that depends on both the pressure gradient and the velocity ratio [Eq. (28)]; k' is always positive. Figure 7a shows that ℓ can be positive or negative depending on the sign of $C_{P\infty}$ and whether $R_0 > 1$ (solid line) or $R_0 < 1$ (dotted line). Figure 7b shows that the overall growth rate of the layer (i.e., $k' + \ell$) increases with $C_{P\infty}$ when $R_0 < 1$ (dotted line) and decreases when $R_0 > 1$ (solid line). Therefore, the reversal in the

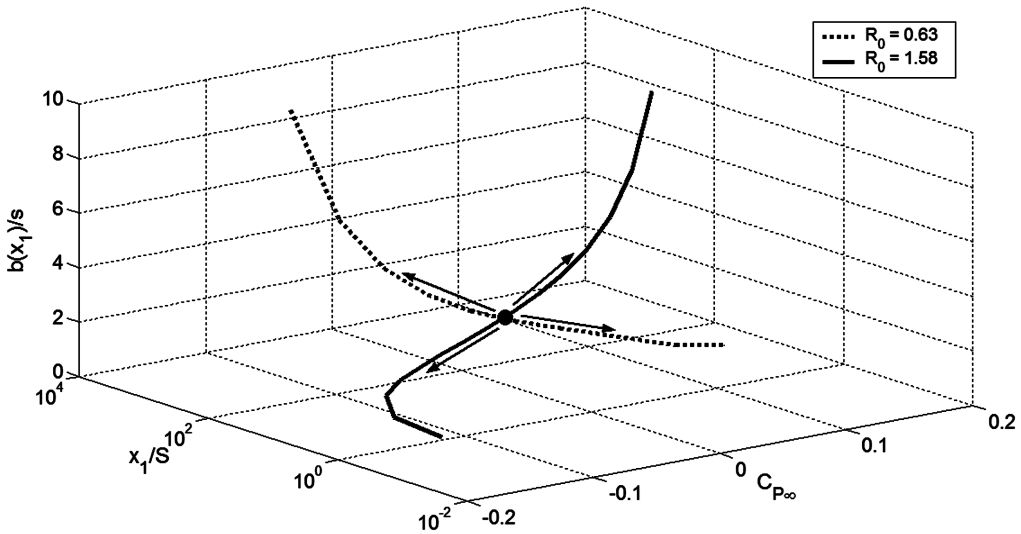

Fig. 6 Nondimensional shear-layer impingement thickness $b(x_1)/s$ versus nondimensional initial region length x_1/s and nondimensional pressure gradient $C_{P\infty}$ for a wall-jet film ($R_0 = 0.63$) and a core-driven film ($R_0 = 1.58$) at TR $= 0.71$.

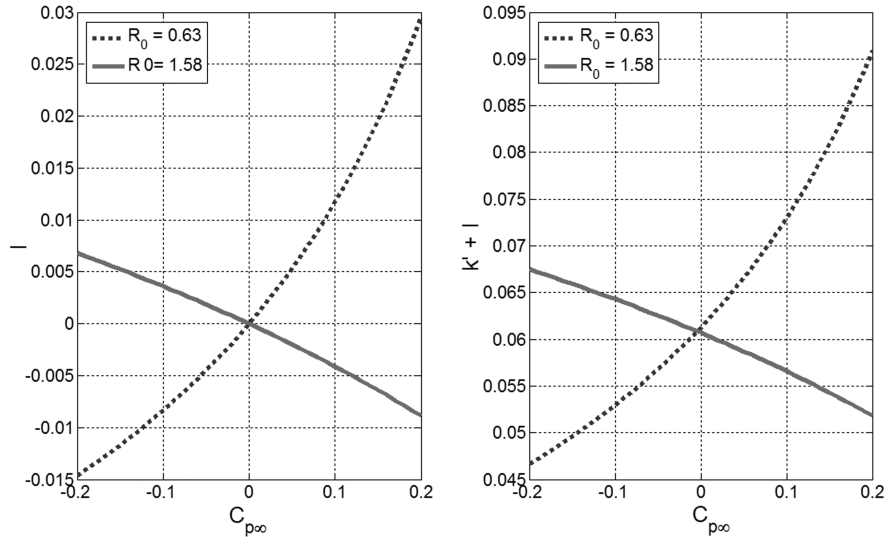

Fig. 7 Shear-layer growth rate: a) change in growth rate due to the presence of a pressure gradient ℓ, and b) overall growth rate $k' + \ell$ versus nondimensional pressure gradient.

effect of the pressure gradient with R arises directly from the influence of the pressure gradient on the shear-layer growth rate.

B. Variable Pressure Gradient Case

In the preceding analysis and results, $C_{P\infty}$ was used to represent a specified constant pressure gradient. However, in situations where the pressure gradient changes with downstream distance (like in a rocket nozzle), it is more common to represent pressure gradients acting on boundary or shear layers using Kays's acceleration parameter K_p [16]. It is defined as follows:

$$K_p = \frac{\nu_\infty}{U_{0,\infty}^2}\frac{\mathrm{d}U_\infty}{\mathrm{d}x} \tag{37}$$

where ν_∞ is the kinematic viscosity of the hot stream, $U_{0,\infty}$ and U_∞ are the initial and local hot-stream velocities, respectively, and x is the downstream distance. K_p is related to $C_{P\infty}$ as follows:

$$K_p = \frac{\nu_\infty}{U_{0,\infty}}\frac{[\sqrt{1-(C_{P\infty}/R_0^2)}-1]}{x} \tag{38}$$

Rearrangement of Eq. (38) provides an expression for $C_{P\infty}$ in terms of K_p that, in conjunction with Eqs. (33) and (34) and Eqs. (1–16), can be used to predict the variation of film-cooling effectiveness under conditions where the streamwise pressure variation is not uniform.

Figure 8 shows film-cooling effectiveness as a function of nondimensional downstream distance for a turbulent core-driven film with three different acceleration parameters. $K_p = -0.22 \times 10^{-6}$ corresponds to a mild adverse variable pressure gradient (MAPG), $K_p = 2.62 \times 10^{-6}$ corresponds to a strong favorable variable pressure gradient (SFPG), and $K_p = 0$ corresponds to a constant zero-pressure gradient (ZPG). The blowing ratio M is 0.33 and the temperature ratio (TR) is 0.86. The solid line shows the model's predictions for a constant ZPG, the dotted line shows the model's predictions for the MAPG, and the dashed line shows the predictions for the SFPG. The symbols show the corresponding experimental data from Teekaram et al. [3]. Despite the relatively weak influence of pressure gradient, the model captures the effect of K_p on effectiveness and matches the magnitude with an average discrepancy of less than 17.5%. Some of the discrepancy between the MSM and Teekaram et al.'s measurement may be attributable to the uncertainty in the turbulence conditions that were estimated earlier. A significant portion of the discrepancy, however, may be attributable to other physical effects, like compressibility, that are not accounted for in the MSM. Compressibility is expected to be important here because the hot-stream flow Mach numbers reported by Teekaram et al.'s experiments were between Mach 0.5 and 0.6.

C. Use of Modified Simon Model to Reconcile Anomalies Present in Literature

One challenge in interpreting previous experimental measurements of film cooling under variable pressure gradient conditions is reconciling apparent contradictions. For instance, Kruse [7] predicts that a favorable pressure gradient degrades film-cooling performance, whereas Kim et al. [17] predicts that it enhances performance. Which is correct? The predictions of the MSM model outlined earlier show that both are correct because Kruse's experiment [7] used a core-driven film ($R > 1$), whereas Kim et al.'s experiment [17] used a wall-jet film ($R < 1$). This trend is confirmed by a more comprehensive analysis of data from ten studies [3,7,17–24] presented in Fig. 9. The filled symbols correspond to 2-D slot injection studies, whereas the open symbols correspond to data from 3-D hole injection studies. The lower plane in the figure shows acceleration parameter and velocity ratio, while the z axis shows the change in film-cooling performance relative to the peak effectiveness at the baseline zero-pressure gradient case. According to the MSM model whose predictions are summarized in Table 2, the data should group into four octants: enhanced cooling performance when $K_p > 0$ and $R < 1$, enhanced cooling performance when $K_p < 0$ and $R > 1$,

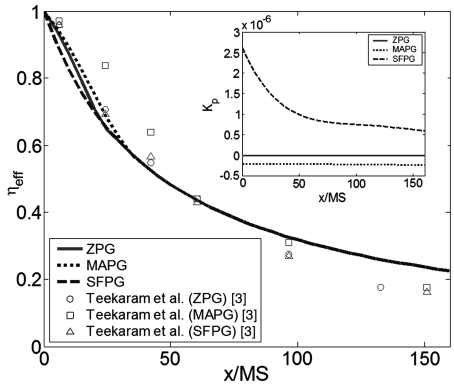

Fig. 8 Film-cooling efficiency η_{eff} predicted by the MSM as a function of nondimensional streamwise distance x/Ms for a turbulent core-driven film ($R_0 = 3.53$) with a strong favorable pressure gradient ($K_p = 2.62 \times 10^{-6}$), a mild adverse pressure gradient ($K_p = -0.22 \times 10^{-6}$), and zero-pressure gradient; $M = 0.33$ and TR $= 0.86$.

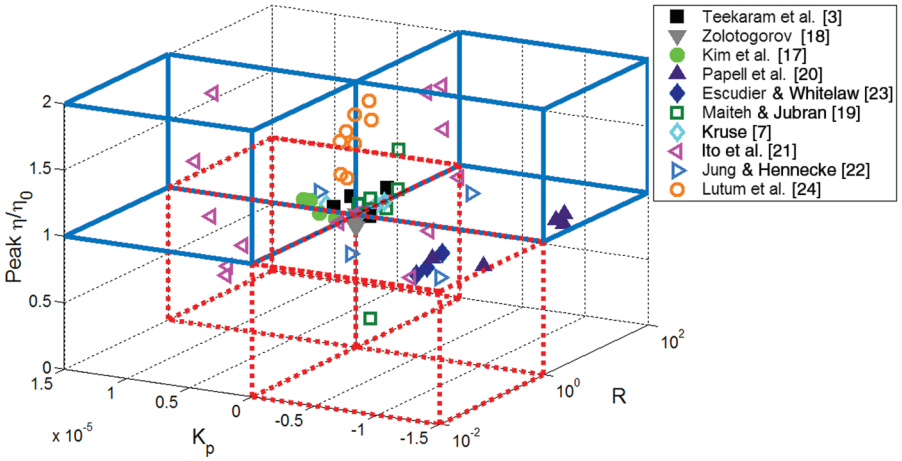

Fig. 9 Peak nondimensional film-cooling effectiveness as a function of acceleration parameter *Kp* and velocity ratio *R* reported in various studies.

degraded cooling performance when $K_p < 0$ and $R < 1$, and degraded cooling performance when $K_p > 0$ and $R > 1$.

These octants are highlighted in Fig. 9. The boxes outlined by the dotted red lines in Fig. 9 show the regions associated with degraded film-cooling performance, and the boxes outlined by the solid blue lines show the regions associated with enhanced film-cooling performance. The MSM model predicts that the remaining four octants should be vacant. This means that, for a specified K_p and R, only an increase *or* a decrease in effectiveness is possible according to the MSM model, not both. Because Fig. 9 shows that most of the experimental data lie within the four octants predicted by the MSM model, the model appears to capture the impact of K_p and R on film-cooling effectiveness in a way that is consistent with most experimental measurements.

Interestingly, Fig. 9 shows that the model correlates both 2-D (solid symbols) and 3-D hole (open symbols) injection data despite the fact that the model was derived for 2-D configurations. This makes sense because the row of holes in a film-cooling application is designed so that the individual fluid jets merge quickly to form an approximately two-dimensional layer that spans and protects the surface. The ability of the jets to merge to form the film depends on, among other things, the hole spacing and the number of rows. Table 3 shows that the hole spacing in four of the five 3-D injection studies reported in Fig. 9 is relatively small ($p/d \leq 4$) indicating that the jets would be able to merge quickly into an approximately 2-D film. It also shows that one of the two data sets that is not correlated by the model (Lutum et al. [24]) corresponds to a single row of holes and the largest p/d, where one would expect it to be more difficult for individual jets to coalesce into a film. Therefore, this result indicates that the model can also be applied to "realistic" 3-D injection geometries, provided the holes are configured in a way that actually produces a film.

Table 2 Summary of MSM predictions

	$K_p < 0$	$K_p > 0$
$R < 1$	$\eta_{\text{eff}}/\eta_{\text{eff},0} < 1$	$\eta_{\text{eff}}/\eta_{\text{eff},0} > 1$
$R > 1$	$\eta_{\text{eff}}/\eta_{\text{eff},0} > 1$	$\eta_{\text{eff}}/\eta_{\text{eff},0} < 1$

Table 3 Summary of 3-D hole injection data

Study	p/d	Spacing type	No. of rows
Kruse [7]	1.5	Small	2
Maiteh and Jubran [19]	2	Small	2
Ito et al. [21]	3	Moderate	1
Jung and Hennecke [22]	4	Moderate	2
Lutum et al. [24]	3 and 6	Moderate–large	1

Two studies [23,24] do not fit the pattern predicted by the MSM. The first, by Escudier and Whitelaw [23], examined film-cooling effectiveness of a core-driven film under a very strong adverse pressure gradient and concluded that an adverse pressure gradient degrades film-cooling performance. However, in these experiments, the pressure gradients were so strong that the flow separated: a condition not accounted for in the MSM and one that is generally avoided in film-cooling applications because it substantially decreases the performance of the film. The second study, by Lutum et al. [24], investigated film-cooling performance of both wall-jet films and core-driven films on a concave surface with zero and favorable pressure gradients ($K_p = 1.0 \times 10^{-6}$). It reported that favorable pressure gradients improved film-cooling performance in both wall-jet films and core-driven films. However, different turbulence intensities were used for the zero ($I_{v,\infty} = 9\%$) and favorable pressure gradient ($I_{v,\infty} = 6\%$) cases. Because the turbulence intensity has a very strong influence on cooling performance, this fact alone could be responsible for the deviation from the model. The authors also introduced an arbitrary scaling factor which further complicates interpretation of the results. Finally, as indicated earlier, the study used a single row of relatively widely spaced holes that would have more difficulty coalescing into a film that would be well approximated by the 2-D model.

V. Conclusions

Simon's [9] semi-empirical wall-jet film-cooling model has been extended to include the effect of variation in the mainstream pressure gradient. The model predicts that the response of a cooling film to the pressure gradient depends upon the freestream-to-film velocity ratio R. For wall-jet films ($R > 1$), an adverse pressure gradient decreases cooling performance, whereas a favorable pressure gradient improves performance. For core-driven films ($R < 1$), the effect is reversed: an adverse pressure gradient improves performance, whereas a favorable pressure gradient decreases it. This reversal is caused by the pressure gradient's influence on the shear-layer growth rate which, in turn, influences its thickness and impingement point. In wall-jet films, a favorable pressure gradient decreases the shear-layer growth rate, thereby moving the impingement point downstream and increasing the shear-layer thickness. This increases the cooling effectiveness. In core-driven films, a favorable pressure gradient decreases the shear-layer growth rate, moves the impingement point upstream, and reduces the shear-layer thickness, thereby reducing cooling effectiveness. The model's predictions resolve most of the discrepancies in the literature regarding the effect of the pressure gradient on film-cooling performance and correlate both 2-D slot and 3-D hole injection data. The latter is possible only when the hole injection scheme is well designed, that is, that the individual jets merge into a film rapidly. This occurs when the hole spacing is small enough ($p/d \leq 4$) and/or if multiple rows of holes are used.

Acknowledgments

This work has been sponsored by the Space Vehicles Technology Institute, Grant NCC3-989, one of the NASA University Institutes, with joint sponsorship from the U.S. Department of Defense. Appreciation is expressed to Claudia Meyer of the NASA Glenn Research Center, program manager of the University Institute activity, and to John Schmisseur and Walter Jones of the U.S. Air Force Office of Scientific Research.

References

[1] Metzger, D., "Cooling Techniques for Gas Turbine Airfoils: A Survey," AGARD CPP-391, 1985.

[2] Goldstein, R., and Jin, P., "Film Cooling Downstream of a Row of Discrete Holes with Compound Angle," *Journal of Turbomachinery*, Vol. 123, No. 2, 2001, pp. 222–230. doi:10.1115/1.1344905

[3] Teekaram, A., Forth, C., and Jones, T., "Film Cooling in the Presence of Mainstream Pressure Gradients," *Journal of Turbomachinery*, Vol. 113, No. 3, 1991, pp. 484–492. doi:10.1115/1.2927900

[4] Hartnett, J., Birkebak, R., and Eckert, E., "Velocity Distributions, Temperature Distributions, Effectiveness and Heat Transfer for Air Injected Through a Tangential Slot into a Turbulent Boundary Layer," *Journal of Heat Transfer*, Vol. 83, Aug. 1961, pp. 293–306.

[5] Pai, B., and Whitelaw, J., "The Influence of Strong Favorable Pressure Gradients on Film-Cooling Effectiveness," Imperial College, Rept. EHT/TN/A/15, 1969.

[6] Hay, N., Lampard, D., and Saluja, C., "Effects of the Condition of the Approach Boundary Layer and of Mainstream Pressure Gradient on the Heat Transfer Coefficient on Film-Cooled Surfaces," *Journal of Engineering for Gas Turbines and Power*, Vol. 107, No. 1, 1985, pp. 99–104.

[7] Kruse, H., "Effects of Hole Geometry, Wall Curvature and Pressure Gradient on Film Cooling Downstream of a Single Row," AGARD CPP-391, 1985.

[8] Goradia, S., and Colwell, G., "Parametric Study of a Two-Dimensional Turbulent Wall Jet in a Moving Stream with Arbitrary Pressure Gradient," *AIAA Journal*, Vol. 9, No. 11, 1971, pp. 2156–2165. doi:10.2514/3.6489

[9] Simon, F., "Jet Model for Slot Film Cooling with Effect of Free-Stream and Coolant Turbulence," NASA TP-2655, 1986.

[10] Abramovich, G., *The Theory of Turbulent Jets*, MIT Press, Cambridge, MA, 1963.

[11] Cruz, C., Raffan, F., Cadou, C., and Marshall, A., "Characterizing Slot Film Cooling Through Detailed Experiments," *Proceedings of the International Mechanical Engineering Conference and Exposition*, American Society of Mechanical Engineers, Fairfield, NJ, Nov. 2006, pp. 507–516.

[12] Sturgess, G., "Account of Film Turbulence for Prediction of Effectiveness from Film Cooling Injection Geometries of a Practical Nature," *Journal of Combustion and Heat Transfer in Gas Turbine Systems*, Vol. 11, edited by E. R. Norster, Permagon Press, Oxford, England, U.K., 1971, pp. 229–250.

[13] Juhasz, A., and Marek, C., "Combustor Liner Film Cooling in the Presence of High Free Stream Turbulence," NASA TN D-6360, 1971.

[14] Stollery, J., and El-Ehwany, A., "A Note on the Use of a Boundary-Layer Model to Correlate Film-Cooling Data," *International Journal of Heat and Mass Transfer*, Vol. 8, No. 1, 1965, pp. 55–65. doi:10.1016/0017-9310(65)90097-9

[15] Ko, S., and Liu, D., "Experimental Investigation on Effectiveness, Heat Transfer Coefficient, and Turbulence of Film Cooling," *AIAA Journal*, Vol. 18, No. 8, Aug. 1980, pp. 907–913. doi:10.2514/3.50833

[16] Kays, W., and Crawford, M., *Convective Heat and Mass Transfer*, 2nd ed., McGraw–Hill, New York, 1980.

[17] Kim, Y., Coon, C., and Moon, H., "Film-Cooling Characteristics of Pressure-Side Discharge Slots in an Accelerating Mainstream Flow," *Proceedings of the ASME Gas Turbine Exposition*, American Society of Mechanical Engineers, Fairfield, NJ, July 2005, pp. 889–897.

[18] Zolotogorov, M., "A Study Concerning the Efficiency of Film Cooling Under Real Conditions in Various Moving Systems," *Journal of Engineering Physics and Thermophysics*, Vol. 22, No. 1, Jan. 1972, pp. 31–33. doi:10.1007/BF00838375

[19] Maiteh, B., and Jubran, B., "Effects of Pressure Gradient on Film Cooling Effectiveness from Two Rows of Simple and Compound Angle Holes in Combination," *Energy Conversion and Management*, Vol. 45, Nos. 9–10, 2004, pp. 1457–1469. doi:10.1016/j.enconman.2003.09.007

[20] Papell, S., Graham, R., and Cageao, R., "Influence of Coolant Tube Curvature on Film Cooling Effectiveness as Detected by Infrared Imagery," NASA TP-1546, Nov. 1979.

[21] Ito, S., Goldstein, R., and Eckert, E., "Film Cooling of a Gas Turbine Blade," *Journal of Engineering for Power*, Vol. 100, No. 3, July 1978, pp. 476–481.

[22] Jung, K., and Hennecke, D., "Curvature Effects on Film Cooling with Injection Through Two Rows of Holes," *Proceedings of the RTO/AVT Symposium on Advanced Flow Management, Part B: Heat Transfer and Cooling in Propulsion and Power Systems*, NATO RTO-MP-69, March 2003, pp. 1–14.

[23] Escudier, M., and Whitelaw, J., "The Influence of Strong Adverse Pressure Gradients on the Effectiveness of Film Cooling," *International Journal of Heat and Mass Transfer*, Vol. 11, No. 8, 1968, pp. 1289–1292. doi:10.1016/0017-9310(68)90198-1

[24] Lutum, E., von Wolfersdorf, J., Semmler, K., Dittmar, J., and Weigand, B., "An Experimental Investigation of Film Cooling on a Convex Surface Subjected to Favorable Pressure Gradient Flow," *International Journal of Heat and Mass Transfer*, Vol. 44, No. 5, 2001, pp. 939–951. doi:10.1016/S0017-9310(00)00158-7